

begindocument/before

## $\gamma$ and $\chi_{c0}$ production in electron-positron annihilation

Shashank Bhatnagar and Vaishali Guleria

*Department of Physics, Chandigarh University, Mohali-140413, INDIA*

### Introduction

Quarkonium production processes are of immense theoretical and experimental interest. In this work we focus on production processes,  $e^- + e^+ \rightarrow \gamma^* \rightarrow \gamma + H$  at center of mass energies,  $\sqrt{s} = 10.6$  GeV, and 4.6 GeV, that proceed through a virtual photon, where  $H$  is a heavy quarkonium of charge conjugation parity,  $C = +1$ . Here,  $H$  can be S-wave spin singlet states such as  $\eta_c(nS)$ ,  $\eta_b(nS)$ , or P-wave spin triplet states such as,  $\chi_{cJ}$  and  $\chi_{bJ}$ , with ( $J = 0, 1, 2$ ). And very recently, the experimental study of the  $e^- e^+ \rightarrow \gamma \chi_{c0,1,2}$ [2] processes was carried at center-of-mass energies ranging from  $\sqrt{s} = 4.008 - 4.6$  GeV using data samples corresponding to an integrated luminosity of  $16 fb^{-1}$  accumulated with the BESIII detector at the BEPCII collider. The production cross sections of  $e^- e^+ \rightarrow \gamma \chi_{c0,c1}$  at each center of mass energy was measured, and the cross section for these processes,  $\sigma(e^- e^+ \rightarrow \gamma \chi_{c0}) = 2.6 \times 10^3$  fb, and  $\sigma(e^- e^+ \rightarrow \gamma \chi_{c1}) = (1.7^{+0.8} \pm 0.2) \times 10^3$  fb at  $\sqrt{s} = 4.5995$  GeV, using integrated luminosity of  $19.3 fb^{-1}$  was reported by BESIII at BEPCII.

$$e^- e^+ \rightarrow \gamma \rightarrow \gamma \chi_{c0}$$

To calculate the above mentioned processes, we will make use of the calculational techniques involved in the quark-triangle diagrams that were recently used for the study of  $M1$  and  $E1$  radiative transitions involving heavy-light quarkonia, such as:  $1^{--} \rightarrow 0^{-+} \gamma$ ,  $0^{-+} \rightarrow 1^{--} \gamma$ [3, 4], and  $1^{+-} \rightarrow 0^{-+} \gamma$ ,  $0^{-+} \rightarrow 1^{+-} \gamma$ [4], besides transitions such as:  $0^{++} \rightarrow 1^{--} \gamma$  and  $1^{--} \rightarrow 0^{++} \gamma$ [3]. We have made use of the generalized method[3, 4] of handling such quark triangle diagrams in the framework of  $4 \times 4$  BSE under Covariant Instantaneous ansatz, which ensures that after the pole integration over the fourth (longitudinal) compo-

nent ( $Md\sigma$ ) of internal hadron momentum,  $q$  is carried out, the effective 3D form of amplitude is still relativistically covariant.

We consider both the  $s$ -channel diagrams in Fig.1 for the process,  $e^- + e^+ \rightarrow \gamma^* \rightarrow \gamma + \chi_{c0,c1}$ , and calculate the contributions of both these diagrams to cross section. Here,  $e^- e^+$  of momenta  $\bar{p}_1$  and  $\bar{p}_2$  annihilate to produce a virtual photon of momentum,  $k' = \bar{p}_1 + \bar{p}_2$ , whose coupling to  $c\bar{c}$  meson and photon is through the quark loop diagram as in Fig.1. These diagrams involve three electromagnetic vertices, and one non-perturbative strong vertex, which involve parity,  $P$  and charge conjugation,  $C$  conservation. Here, the photon-quark-anti-quark vertex is given as  $ie_Q \gamma_\mu$ , where,  $e_Q = \frac{2}{3}e$  is the charge of the  $c$  quark.

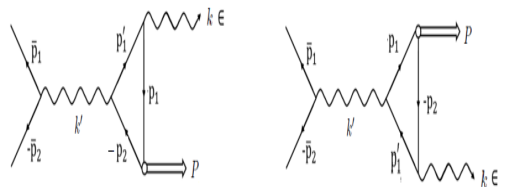


FIG. 1: Lowest order  $s$ -channel Feynman diagrams for the production of  $\gamma$  and  $\chi_{cJ}$  ( $J = 0, 1$ ) in electron-positron annihilation. The exchange diagram on the right is obtained from the diagram on the left by reversing the direction of internal fermionic lines.

For the diagrams in Fig.1, the invariant amplitude  $M_{fi}^1$  for the first diagram on the left is

given by the one-loop momentum integral as:

$$M_{fi}^1 = iee_Q^2 [\bar{v}^{(s2)}(\bar{p}_2)\gamma_\mu u^{(s1)}(\bar{p}_1)] \times \frac{1}{s} \int \frac{d^4 q}{(2\pi)^4} Tr[\bar{\Psi}_S(P, q)\epsilon^\lambda' S_F(p'_1)\gamma_\mu].$$

where,  $P, q$  are the external momentum and internal momentum of  $\chi_{c0}$ , with 4D BS wave function,  $\Psi_S(P, q)$ , while,  $k$  and  $\epsilon^\lambda'$ , are the momentum and the polarization vector of the emitted photon, and in the center of mass frame, we have expressed  $\bar{p}_1 + \bar{p}_2 = \sqrt{s}$ . The second diagram is obtained from the first diagram by reversing the direction of internal fermion lines, which amounts to exchange of final states. The amplitude from the second diagram is equal to the amplitude from the first diagram. The wave functions of both incoming and outgoing particles are normalized to one particle per unit volume. The wave functions for equal mass scalar quarkonia such as  $\chi_{c0}$  can be shown to be reduced to:

$$\Psi_S(\hat{q}) = N_S \left[ \frac{\hat{q}^2}{m} + i\hat{q} + 2\frac{Pq}{M} \right] \phi_S(\hat{q}),$$

where the radial wave functions obtained by analytic solutions of mass spectral equations for scalar meson are

$$\phi_S(1P, \hat{q}) = \sqrt{\frac{2}{3}} \frac{1}{\pi^{3/4}} \frac{1}{\beta_S^{5/2}} |\hat{q}| e^{-\frac{\hat{q}^2}{2\beta_S^2}},$$

$$\phi_S(2P, \hat{q}) = \sqrt{\frac{5}{3}} \frac{1}{\pi^{3/4}} \frac{1}{\beta_S^{5/2}} |\hat{q}| (1 - \frac{2\hat{q}^2}{5\beta_S^2}) e^{-\frac{\hat{q}^2}{2\beta_S^2}},$$

The spin averaged amplitude modulus square,  $|\bar{M}_{fi}|^2 = \frac{1}{4} \sum_{s_1, s_2, \lambda} M_{fi}^\dagger M_{fi}$  is obtained by averaging over the spins of incident particles, and summing over the polarizations of the final photon. We can then express  $|\bar{M}_{fi}|^2$  as [5],

$$|\bar{M}_{fi}|^2 = \left[ 2\beta_1^2(-s+3m_e^2) - \frac{1}{2}\beta_3^2 s^2 (1 - \cos^2\theta) \right],$$

with  $\beta_1$ , and  $\beta_3$  being the form factors with details in [5]. Following a series of steps, we

can express the total cross section for the process as,  $\sigma = \frac{1}{32\pi^2 s^{3/2}} |\vec{P}'| \int d\Omega' |\bar{M}_{fi}|^2$ , with  $|\vec{P}'| = \frac{s-M^2}{\sqrt{s}}$  being the momenta of either of the outgoing particles in the center of mass frame.

TABLE I: Cross sections for processes,  $e^-e^+ \rightarrow \gamma\chi_{c0}(nP)$  ( $n = 1, 2$ ) (in fb) calculated in BSE-CIA at  $\sqrt{s} = 10.6\text{GeV}$ ,  $4.6\text{ GeV}$  and  $4\text{ GeV}$ , along with recent data from Belle[1](at  $10.58\text{ GeV}$ ), BESIII[2] (at  $4.6\text{ GeV}$  and  $4\text{ GeV}$ ), and other models

Processes	$\sqrt{s}$	BSE	Experiment
$e^-e^+ \rightarrow \gamma\chi_{c0}(1P)$	10.6	3,810	$< 205.9$ [1]
$e^-e^+ \rightarrow \gamma\chi_{c0}(1P)$	4.6	46.617	$< 2.6 \times 10^3$ [2]
$e^-e^+ \rightarrow \gamma\chi_{c0}(1P)$	4.0	13.785	$< 4.5 \times 10^3$ [2]
$e^-e^+ \rightarrow \gamma\chi_{c0}(2P)$	10.6	3.570	
$e^-e^+ \rightarrow \gamma\chi_{c0}(2P)$	4.6	64.073	

Our cross sections for the process,  $e^-e^+ \rightarrow \gamma\chi_{c0}$ , at  $\sqrt{s} = 10.6\text{ GeV}$  are consistent with the upper limit of  $\sigma$  estimates by the Belle collaboration at  $< 205.9\text{ fb}$  [1], and can also be compared with the corresponding cross sections of this process obtained in other models[5]. For this process, with decrease in energy, the plot of cross section shows first a continuous rise followed by fall to a value  $46.667\text{ fb}$  at  $4.6\text{ GeV}$ , which is consistent with the upper limit estimates of BESIII[2] collaboration. Further, from our plot of  $\sigma$ , we also notice small fluctuations of order  $5\text{ - }10\text{ fb}$ , in the low energy region  $6\text{ - }4\text{ GeV}$ . To analyze this in [3], we have further drawn the plots of the form factors  $\beta_1$  and  $\beta_3$  (versus  $\sqrt{s}$ ) in the energy region  $12\text{ GeV} - 4\text{ GeV}$ . The fluctuations in cross sections are analyzed in terms of form factors (see Ref.[5] for details).

## References

- [1] S.Jia et al.,(Belle Collaboration), Phys. Rev. D 98, 092015 (2018).
- [2] M.Ablikim et al., Phys. Rev. D 104, 092001 (2021).
- [3] S.Bhatnagar, E.Gebrehana, Phys. Rev. D102, 094024 (2020).
- [4] V.Guleria, E.Gebrehana, S.Bhatnagar, Phys. Rev. D104, 094045 (2021).
- [5] S.Bhatnagar, V.Guleria, arxiv: 2206.02229[hep-ph].